

Directed Peptide Assembly at the Lipid–Water Interface Cooperatively
Enhances Membrane Binding and Activity[†]

Mingming Ma and Dennis Bong*

Department of Chemistry, The Ohio State University, Columbus, Ohio 43210, United States

Received November 6, 2010. Revised Manuscript Received December 9, 2010

We modified membrane-active peptides with synthetic recognition modules to foster peptide assembly at the lipid–water interface. The designed recognition strategy has been previously reported: tris-cyanuric acid and tris-melamine have been found to bind selectively to each another when membrane-anchored. We designed this interaction to occur between two membrane-active peptides, forming a heteromeric complex at the lipid–water interface that exhibits superior membrane binding and permeation compared to the monomeric peptides, presumably because of the higher avidity of the assembled structure. These conjugates do not assemble appreciably in solution but assemble at the lipid–water interface, with surface binding of the peptide acting cooperatively with molecular recognition to yield improved binding and permeation. Furthermore, we find that specific recognition between tris-cyanuric acid phospholipid (TCA-PE) at low surface concentration and tris-melamine magainin (TMM) or hexa-melamine magainin (HMM) results in highly lytic binding, whereas no binding is detectable in the absence of lipid recognition. These findings suggest a noncovalent strategy to enhance peptide membrane activity, which may lead to the discovery of more potent surface-active agents such as antimicrobials.

Introduction

Lipid self-assembly into bilayer membranes is one the earliest known examples of functional noncovalent chemistry.¹ Lipid membranes not only organize lipid molecules but also provide a medium in which to further organize and facilitate the chemistry of “guest” molecules that are imbedded within the membrane or transiently bound to the surface.² Biological membranes are very heterogeneous and so packed with proteins that the line between “host” and “guest” is indistinct; this heterogeneity potentially disconnects synthetic model membrane systems from living membranes.³ Concepts that are general to both synthetic membranes and biomembranes include surface-binding avidity through multivalency and surface-partitioning driven by electrostatics and hydrophobic insertion.⁴ A broad class of cationic antimicrobial peptides play a key role in innate immunity and bind to membranes on the basis of these simple physical principles, without specific molecular recognition between a peptide and a surface.^{5–7} Electrostatically targeted cationic antimicrobial peptides have attracted considerable attention as a potential strategy to circumvent the emergence of antibiotic resistance through the use of a nonspecific targeting method.^{8,9} This has led to many synthetic mimics designed to improve potency by limiting enzymatic peptide digestion through the use of

non-native structures, including beta peptides,^{10–13} peptoids,^{14–17} polymers,^{18–21} and small molecules.^{22,23} These approaches have led to an apparent potency ceiling,²⁴ despite improvements observed in proteolytic stability. Indeed, the potency of native antimicrobials limits the majority of these reagents to topical use.²⁵ Natural product antimicrobial peptides that hold exceptional potency include daptomycin^{9,26,27} and nisin,²⁸ daptomycin is currently a marketed antibiotic. These peptides are distinguished not only by their nanomolar potency but also by their specific lipid-binding interactions: most antimicrobials bind electrostatically and exhibit micromolar potency. It is thought that antimicrobial activity derives from the disruption of membrane integrity, which requires peptide aggregation within the

[†] Part of the Supramolecular Chemistry at Interfaces special issue.

*Corresponding author. E-mail: bong@chem.osu.edu.

(1) Cullis, P. R.; Hope, M. J.; Tilcock, C. P. *Chem. Phys. Lipids* **1986**, *40*, 127–144.

(2) Gennis, R. B. *Biomembranes: Molecular Structure and Function*; Springer-Verlag: New York, 1989; p 526.

(3) Chan, Y. H.; Boxer, S. G. *Curr. Opin. Chem. Biol.* **2007**, *11*, 581–587.

(4) Mammen, M.; Chio, S.-K.; Whitesides, G. M. *Angew. Chem., Int. Ed.* **1998**, *37*, 2755–2794.

(5) Beutler, B. *Mol. Immunol.* **2004**, *40*, 845–859.

(6) Finlay, B. B.; Hancock, R. E. W. *Nat. Rev. Microbiol.* **2004**, *2*, 497–504.

(7) Vivier, E.; Malissen, B. *Nat. Immunol.* **2005**, *6*, 17–21.

(8) Zasloff, M. *Nature* **2002**, *415*, 389–395.

(9) Vooturi, S. K.; Firestone, S. M. *Curr. Med. Chem.* **2010**, *17*, 2292–2300.

(10) Porter, E. A.; Wang, X.; Lee, H.-S.; Weisblum, B.; Gellman, S. H. *Nature* **2000**, *404*, 565.

(11) Karlsson, A. J.; Pomerantz, W. C.; Neilsen, K. J.; Gellman, S. H.; Palecek, S. P. *ACS Chem. Biol.* **2009**, *4*, 567–579.

(12) Koyack, M. J.; Cheng, R. P. *Methods Mol. Biol.* **2006**, *340*, 95–109.

(13) Frackenhohl, J.; Arvidsson, P. I.; Schreiber, J. V.; Seebach, D. *ChemBioChem* **2001**, *2*, 445–455.

(14) Patch, J. A.; Barron, A. E. *Curr. Opin. Chem. Biol.* **2002**, *6*, 872–877.

(15) Patch, J. A.; Barron, A. E. *J. Am. Chem. Soc.* **2003**, *125*, 12092–12093.

(16) Yoo, B.; Kirshenbaum, K. *Curr. Opin. Chem. Biol.* **2008**, *12*, 714–721.

(17) Zuckermann, R. N.; Kodadek, T. *Curr. Opin. Mol. Ther.* **2009**, *11*, 299–307.

(18) Mowery, B. P.; Lee, S. E.; Kissounko, D. A.; Epand, R. F.; Epand, R. M.; Weisblum, B.; Stahl, S. S.; Gellman, S. H. *J. Am. Chem. Soc.* **2007**, *129*, 15474–15476.

(19) Epand, R. F.; Mowery, B. P.; Lee, S. E.; Stahl, S. S.; Lehrer, R. I.; Gellman, S. H.; Epand, R. M. *J. Mol. Biol.* **2008**, *379*, 38–50.

(20) Kenawy el, R.; Worley, S. D.; Broughton, R. *Biomacromolecules* **2007**, *8*, 1359–1384.

(21) Tew, G. N.; Liu, D.; Chen, B.; Doerksen, R. J.; Kaplan, J.; Carroll, P. J.; Klein, M. L.; DeGrado, W. F. *Proc. Natl. Acad. Sci. U.S.A.* **2002**, *99*, 5110–5114.

(22) Tew, G. N.; Scott, R. W.; Klein, M. L.; DeGrado, W. F. *Acc. Chem. Res.* **2010**, *43*, 30–39.

(23) Yang, L.; Gordon, V. D.; Trinkle, D. R.; Schmidt, N. W.; Davis, M. A.; DeVries, C.; Som, A.; Cronan, J. E., Jr.; Tew, G. N.; Wong, G. C. *Proc. Natl. Acad. Sci. U.S.A.* **2008**, *105*, 20595–20600.

(24) Porter, E. A.; Weisblum, B.; Gellman, S. H. *J. Am. Chem. Soc.* **2005**, *127*, 11516–11529.

(25) Dai, T.; Huang, Y. Y.; Sharma, S. K.; Hashmi, J. T.; Kurup, D. B.; Hamblin, M. R. *Recent Pat. Anti-Infect. Drug Discov.* **2010**, *5*, 124–151.

(26) Baltz, R. H. *Curr. Opin. Chem. Biol.* **2009**, *13*, 144–151.

(27) Wang, J. L.; Hsueh, P. R. *Expert Opin. Pharmacother.* **2009**, *10*, 785–796.

(28) Chatterjee, C.; Paul, M.; Xie, L.; Van der Donk, W. A. *Chem. Rev.* **2005**, *105*, 633–683.

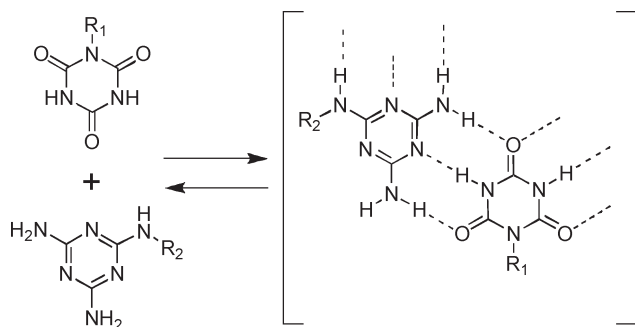
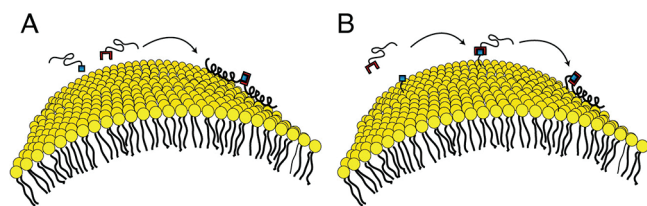


Figure 1. Illustration of hydrogen bonding patterns observed with derivatives of cyanuric acid (top left) and melamine (bottom left) in organic solvents and the solid state.

Scheme 1. Recognition-Assisted Membrane Binding^a



^a (A) Two peptides bind to each other in the presence of the membrane, enhancing partitioning. (B) Specific lipid recognition by a peptide similarly enhances insertion into the membrane.

membrane. With electrostatic binding, high concentration is required to drive aggregation within the membrane;²⁹ it is possible that specific lipid-binding interactions decrease the threshold for assembly (activity) within the membrane, thereby increasing potency.

We explored this idea by the installation of recognition motifs on antimicrobial peptide magainin and probed whether a system predisposed to assembly either through peptide–peptide interactions or peptide–lipid interactions would yield improved membrane activity (Scheme 1). Our prior work indicated that molecular recognition between membrane-anchored cyanuric acid and melamine groups was robust and selective at the lipid–water interface,^{30,31} despite exposure to a competitive aqueous solvent.³² Furthermore, selective binding interactions at the membrane were observed between appropriately functionalized peptides and lipids even at surface concentrations of 0.1–1%. Though the size of the assemblies formed precluded facile detailed characterization, the selectivity of the pairwise interaction between cyanuric acid and melamine is consistent with specific hydrogen bond pattern recognition established in organic solvents and the

solid state (Figure 1).^{33–43} There are few synthetic recognition motifs compatible with aqueous solvents,^{44–47} thus we employed cyanuric acid/melamine binding in our study of peptide assembly and activity at the lipid–water interface; a number of recognition motifs at the lipid–water interface have been explored by us and others.^{47–53} We synthesized magainin peptide variants conjugated to tris- and hexa-cyanuric acid (TCAM and HCAM) as well as tris- and hexa-melamine (TMM and HMM) modules (Figure 2) and studied their membrane activity in isolation and in concert. Magainins are natural antimicrobial peptides extracted from frog skin.^{8,54} We chose magainin to model noncovalently guided peptide–membrane interactions because magainin membrane binding has been extensively studied and its mode of interaction with synthetic membranes is largely understood;^{29,55–59} thus one may clearly observe the influence of molecular recognition on its known behavior. Cationic at physiological pH, random coil magainin peptides selectively bind lipid membranes with high negative zeta potentials, insert into the membrane, and fold into an α helix. The mechanism of lipid membrane destruction by magainin is described by a toroidal-pore model.⁶⁰ It is thought that when the concentration of magainin on the lipid membrane reaches a threshold, several magainin molecules will aggregate and form a transient ion channel. We covalently attached CA/M recognition motifs to magainin peptides and found that these new conjugates can bind lipid membranes with a low negative zeta potential in a cooperative manner that requires both partners as well as the membrane. We additionally find that the direct CA/M recognition between peptide and lipid results in similar increases in peptide membrane activity.

Experimental Section

Vesicle Preparation. Large unilamellar vesicles (LUVs) were prepared by the buffer hydration of dried lipid films followed by extrusion.^{61,62} Dye-encapsulating LUVs were prepared by the hydration of films with 50 mM sodium phosphate buffer at pH 6.8 containing calcein or carboxyfluorescein dye at the desired concentration of 51 mM. Carboxyfluorescein-containing LUVs were prepared at pH 7.4. Hydrated lipid suspensions were extruded

- (29) Oren, Z.; Shai, Y. *Biopolymers* **1998**, *47*, 451–63.
 (30) Ma, M.; Gong, Y.; Bong, D. *J. Am. Chem. Soc.* **2009**, *131*, 16919–16926.
 (31) Ma, M.; Paredes, A.; Bong, D. *J. Am. Chem. Soc.* **2008**, *130*, 14456–14458.
 (32) Oshovsky, G. V.; Reinhoudt, D. N.; Verboom, W. *Angew. Chem., Int. Ed.* **2007**, *46*, 2366–2393.
 (33) ten Cate, M. G. J.; Huskens, J.; Crego-Calama, M.; Reinhoudt, D. N. *Chem.—Eur. J.* **2004**, *10*, 3632–3639.
 (34) Damodaran, K.; Sanjayan, G. J.; Rajamohanam, P. R.; Ganapathy, S.; Ganesh, K. N. *Org. Lett.* **2001**, *3*, 1921–1924.
 (35) Ranganathan, A.; Pedireddi, V. R.; Rao, C. N. R. *J. Am. Chem. Soc.* **1999**, *121*, 1752–1753.
 (36) Mammen, M.; Shakhovich, E. I.; Deutch, J. M.; Whitesides, G. M. *J. Org. Chem.* **1998**, *63*, 3821–3830.
 (37) Cheng, X.; Gao, Q.; Smith, R. D.; Simanek, E. E.; Mammen, M.; Whitesides, G. M. *J. Org. Chem.* **1996**, *61*, 2204–2206.
 (38) Zerkowski, J. A.; MacDonald, J. C.; Seto, C. T.; Wierda, D. A.; Whitesides, G. M. *J. Am. Chem. Soc.* **1994**, *116*, 2382–2391.
 (39) Mathias, J. P.; Seto, C. T.; Whitesides, G. M. *Polym. Prepr. (Am. Chem. Soc., Div. Polym. Chem.)* **1993**, *34*, 92–93.

- (40) Seto, C. T.; Whitesides, G. M. *J. Am. Chem. Soc.* **1993**, *115*, 905–916.
 (41) Zerkowski, J. A.; Seto, C. T.; Whitesides, G. M. *J. Am. Chem. Soc.* **1992**, *114*, 5473–5475.
 (42) Seto, C. T.; Whitesides, G. M. *J. Am. Chem. Soc.* **1990**, *112*, 6409–6411.
 (43) Wang, Y.; Wei, B.; Wang, Q. *J. Chem. Crystallogr.* **1990**, *20*, 79–84.
 (44) Brunsveld, L.; Vekemans, J. A.; Hirschberg, J. H.; Sijbesma, R. P.; Meijer, E. W. *Proc. Natl. Acad. Sci. U.S.A.* **2002**, *99*, 4977–4982.
 (45) Brunsveld, L.; Folmer, B. J. B.; Meijer, E. W.; Sijbesma, R. P. *Chem. Rev.* **2001**, *101*, 4071–4098.
 (46) Kawasaki, T.; Tokuhira, M.; Kimizuka, N.; Kunitake, T. *J. Am. Chem. Soc.* **2001**, *123*, 6792–6800.
 (47) Ariga, K.; Kunitake, T. *Acc. Chem. Res.* **1998**, *31*, 371–378.
 (48) Tang, M.; Waring, A. J.; Lehrer, R. I.; Hong, M. *Angew. Chem., Int. Ed.* **2008**, *47*, 3202–3205.
 (49) Menger, F. M.; Zhang, H. *J. Am. Chem. Soc.* **2006**, *128*, 1414–1415.
 (50) Marchi-Artzner, V.; Lehn, J. M.; Kunitake, T. *Langmuir* **1998**, *14*, 6470–6478.
 (51) Gong, Y.; Ma, M.; Luo, Y.; Bong, D. *J. Am. Chem. Soc.* **2008**, *130*, 6196–205.
 (52) Gong, Y.; Luo, Y.; Bong, D. *J. Am. Chem. Soc.* **2006**, *128*, 14430–14431.
 (53) Nowick, J. S.; Chen, J. S. *J. Am. Chem. Soc.* **1992**, *114*, 1107–1108.
 (54) Zasloff, M. *Proc. Natl. Acad. Sci. U.S.A.* **1987**, *84*, 5449–53.
 (55) Wieprecht, T.; Beyermann, M.; Seelig, J. *Biochemistry* **1999**, *38*, 10377–10387.
 (56) Wenk, M. R.; Seelig, J. *Biochemistry* **1998**, *37*, 3909–3916.
 (57) Bechinger, B. *J. Membr. Biol.* **1997**, *156*, 197–211.
 (58) Matsuzaki, K.; Nakamura, A.; Murase, O.; Sugishita, K.-i.; Fujii, N.; Miyajima, K. *Biochemistry* **1997**, *36*, 2104–2111.
 (59) Bechinger, B.; Zasloff, M.; Opella, S. J. *Protein Sci.* **1993**, *2*, 2077–2084.
 (60) Yang, L.; Weiss, T. M.; Lehrer, R. I.; Huang, H. W. *Biophys. J.* **2000**, *79*, 2002–2009.
 (61) Szoka, F. C. *J. Liposome Res.* **1998**, *8*, vii–ix.
 (62) Olson, F.; Hunt, C. A.; Szoka, F. C.; Vail, W. J.; Papahadjopoulos, D. *Biochim. Biophys. Acta* **1979**, *557*, 9–23.

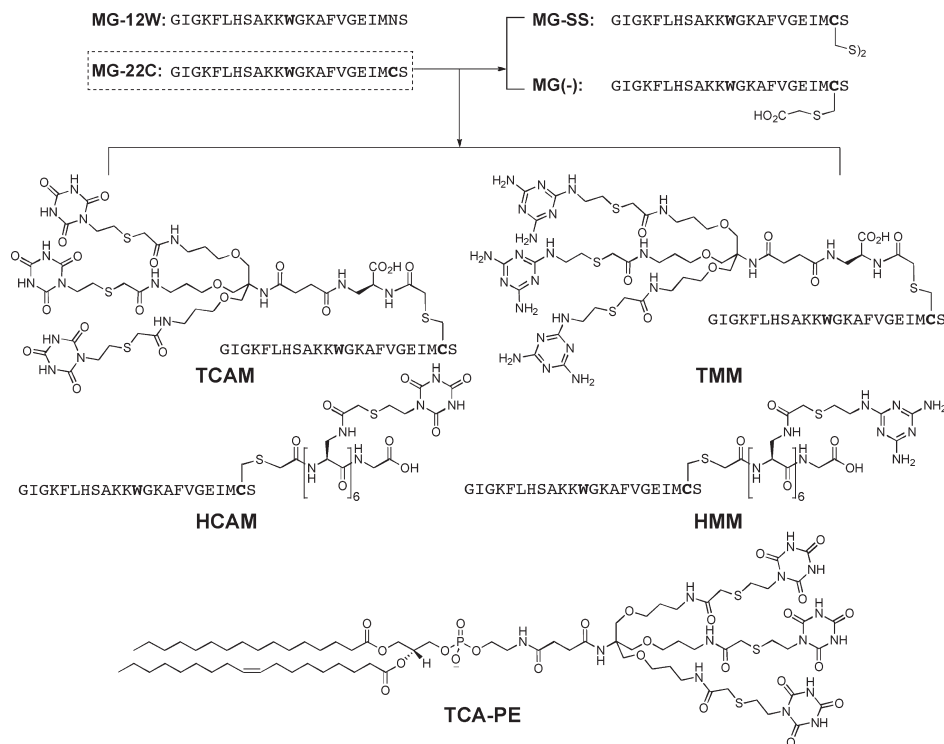


Figure 2. Magainin variant peptides synthesized for this study. All peptides have a free *N* terminus and *C*-terminal amide. Cysteine variant MG-22C was derivatized further at the cysteine side chain to produce the variants shown. The cyanuric acid lipid (TCA-PE) was used to anchor TMM and HMM peptides to the membrane by CA/M recognition.

10 times through a 100 nm polycarbonate filter. Nonencapsulated dye was removed by gel filtration using a Sephadex G-50 column equilibrated with PBS buffer (50 mM sodium phosphate, 120 mM sodium chloride) at pH 6.8 for calcein and pH 7.4 for carboxyfluorescein. The size and zeta potential of the vesicles were measured on a Malvern Instruments zetasizer nano-zs at 25 °C.

Dye Release Assay of Membrane Activity. All measurements were carried out at 25 °C unless otherwise specified. Stock solutions of calcein or Cbf-loaded LUVs with a lipid composition of 10/90 POPG/ePC or 2/98 TCA-PE/ePC were diluted with PBS buffer (50 mM sodium phosphate, 120 mM sodium chloride, pH 6.8 for calcein, pH 7.4 for carboxyfluorescein) to a 50 μ M lipid concentration and a 2 mL volume in a 3 mL fluorescence cuvette. Dye emission (519 nm) was monitored using a Perkin-Elmer LS-50B fluorimeter (excitation 495 nm with a 515 nm cutoff filter). The fluorescence of total dye release (F_{total}) was established by vesicle lysis with 100 μ L of 10% Triton X-100. The dye release percentage was defined as $(F_t - F_i)/(F_{\text{total}} - F_i)$, where F_t is the fluorescence intensity of the sample at different time points and F_i is the fluorescence intensity immediately after peptide addition.

Calculation of Peptide–Membrane Partitioning Coefficients. Titration curves for the calculation of peptide–membrane partitioning coefficients⁶³ were obtained by the treatment of peptide solutions (110 μ L volume, 5 μ M) with LUVs (1 mM 10/90 POPG/ePC) while monitoring tryptophan fluorescence emission from 290 to 400 nm (excitation 275 nm, cutoff filter 290 nm). The ratio of peak intensity for bound and unbound (315 nm/355 nm) was plotted as a function of the lipid/peptide ratio (L/P) and the curve was fitted to determine the convergence value at infinite L/P, which was taken as the saturation point. Emission ratios were converted to fractional binding and surface concentration, X_b . An approximation of the partitioning coefficient K_p that ignores changing surface charge during the titration was obtained by a linear fit of X_b against the free peptide concentration; this

approximation appears to be appropriate given the low surface potential (10% POPG) and roughly linear $X_b/C_{p,\text{free}}$ plot.

Circular Dichroism. Circular dichroism (CD) spectra of peptide/vesicle binding were determined using a Jasco J-815 spectrometer under a nitrogen atmosphere over the range of 195–260 nm at 25 °C. Typically, 0.25 mL of a 15 μ M peptide solution in PBS at pH 6.8 was placed in a 1 mm quartz cuvette and titrated with a 10 mM LUV suspension (10/90 POPG/ePC).

Results and Discussion

Design and Synthesis. Magainin sequences are easily accessed by solid-phase peptide synthesis. We prepared known variants of the native magainin 2 sequence wherein phenylalanine is replaced with tryptophan; this F \rightarrow W variant (MG-12W)⁶⁴ retains activity and has a convenient indole functional group that facilitates concentration determination and the measurement of membrane binding. Variant MG-12W was further modified by the replacement of asparagine with cysteine to permit the selective sulfhydryl side-chain reaction of the unprotected, purified magainin variant in solution while preserving the free *N* terminus found in native magainin sequences. This magainin variant (MG-22C) was used to generate the peptides in this study (Figure 2). The cysteine sulfhydryl was alkylated with hexa- and tris-cyanuric acid and melamine chloroacetyl derivatives, prepared using straightforward synthesis procedures (Supporting Information). Tris-cyanuric acid (TCA) and melamine (TM) modules were derived from tris buffer, and hexa-cyanuric acid (HCA) and -melamine (HM) modules were synthesized by the side-chain derivatization of hexa-peptides. Diaminopropionic acid was used as an anionic linker between peptide and TCA and TM modules to circumvent solubility problems encountered with neutral linkers. Because this alters the overall peptide charge, a magainin

(63) Beschiaschvili, G.; Seelig, J. *Biochemistry* **1990**, *29*, 10995–11000.

(64) Dempsey, C. E.; Ueno, S.; Avison, M. B. *Biochemistry* **2003**, *42*, 402–409.

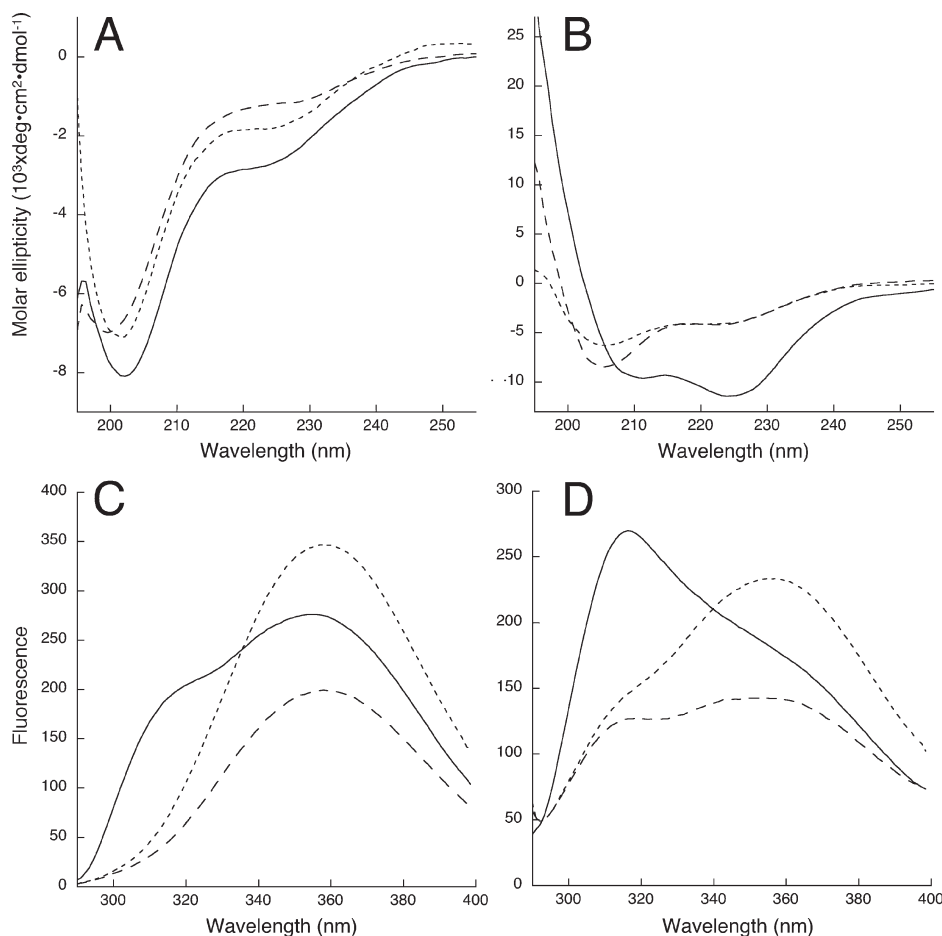


Figure 3. Circular dichroism spectra of TCAM (---), TMM (—), and the equimolar mixture TCAM/TMM (—) in (A) PBS at pH 7.4 and (B) in the same buffer, with 10% POPG/ePC vesicles, at a lipid/peptide ratio of 100:1. Tryptophan fluorescence of the same is shown (C) without lipid and (D) at a lipid/peptide ratio of 100:1.

variant, MG(−), was prepared as an electrostatically identical control in which the cysteine side chain was alkylated with chloroacetic acid. Additionally, air oxidation in basic buffer yielded the disulfide covalent dimer (MG-SS), which was used to compare to noncovalent peptide assemblies at the membrane. Increased antimicrobial potency has been observed with disulfide dimer⁶⁴ MG-SS relative to monomeric magainin, underscoring the importance of the peptide oligomerization state in membrane activity. We additionally studied TMM or HMM peptide binding to tris-cyanuric acid-functionalized lipid TCA-PE. Binding between peptides and lipids functionalized with cyanuric acid and melamine has been previously established,³⁰ but we provide herein a more quantitative analysis of the process.

Cooperative Peptide Membrane Binding and CA/M Recognition. The membrane binding of magainin peptides is largely dependent on complementary electrostatic interactions between a cationic peptide and an anionic surface, with partitioning equilibria increasing with more negative surface potentials. We chose to study the binding of magainin variants with membranes composed of 90% egg phosphatidyl choline (ePC) lipid and 10% phosphatidylglycerol (POPG), which bears a negative charge because of the phosphate headgroup. At 10% negative charge, magainin binding is marginal; the control magainin sequence with an additional carboxylate, MG(−), is even weaker. An examination of TCAM, TMM, and their 1:1 mixture by CD indicated random coil sequences in solution. The addition of 10% POPG LUVs to the peptide samples produced minor changes in the CD spectra of the individual peptides, whereas the mixture showed the

significant development of helicity (Figure 3). It appears that both peptides and a hospitable membrane, are required for helical folding, suggestive of peptide assembly at the membrane. We further monitored changes in tryptophan fluorescence upon treatment with 10% POPG/ePC vesicles. Upon membrane partitioning, it is known that the MG-12W sequence will fold into a helix and bury its hydrophobic face into the lipid matrix, causing a blue shift in Trp fluorescence. This fluorescence assay for membrane binding proved more sensitive than CD. Significantly stronger changes in Trp fluorescence were exhibited by the 1:1 mixture of TCAM/TMM than the individual peptides at equimolar total peptide concentration. Presumably, this is because of molecular recognition between the cyanuric acid and melamine groups. The fluorescence data further indicated the presence of a blue-shifted emission band for the mixture even in the absence of lipid (Figure 3). Thus, it is possible that there is an unstructured heteromeric molten globule state of the two peptides that buries the indole fluorophore without helical CD signatures. Whereas the tryptophan emission intensity varied for all of the magainin variants, generally one could observe that MG(−), TCAM, TMM, HCAM, and HMM exhibit the expected single emission peak at ~355 nm and the spectra of MG-12W, the 1:1 mixture of TCAM/TMM, and disulfide dimer MG-SS all feature an additional blue-shifted shoulder at 315 nm. In the case of disulfide MG-SS, the emission intensity at 315 nm is equal to that found at 355 nm (Figure 4), indicative of substantive solvent exclusion from the tryptophan site and consistent with self-aggregation or intramolecular burial. Treatment with vesicles yields a continued increase

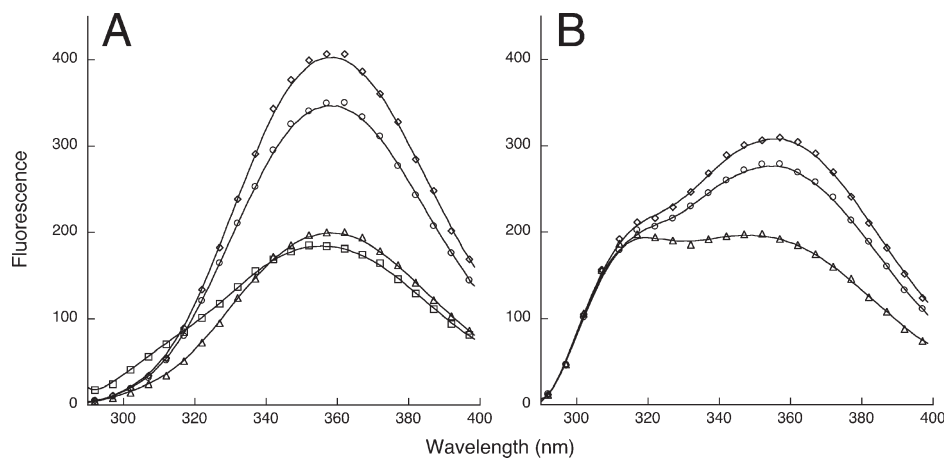


Figure 4. Tryptophan fluorescence spectra in PBS at pH 7.4 of (A) MG(–) (\diamond), TCAM (\circ), TMM (\triangle), and HMM (\square) and (B) MG-12W (\diamond), a TCAM/TMM (\circ) mixture, and MG-SS (\triangle).

in emission intensity at 315 nm, suggesting that membrane partitioning is favored relative to peptide folding or aggregation. However, significant peak broadening was also observed, leading to increased emission at 355 nm as well, making it difficult to assay binding. Tryptophan fluorescence of the remaining peptides was not problematic, permitting a quantitative analysis of surface partitioning.

Calculation of Peptide–Membrane Partitioning Coefficients. We followed the binding of MG(–), TCAM, TMM, and the mixture of TCAM/TMM to 10% POPG/ePC vesicles by the observation of tryptophan fluorescence as a function of lipid concentration. Isolated peptides MG(–), TCAM, and TMM bound weakly to vesicles under these conditions, and it was not possible to approach signal saturation change even at high lipid-to-peptide ratios, prohibiting fitting of the data (Figure 5). In contrast, the 1:1 mixture of TCAM/TMM at the same total peptide concentration partitioned readily into membranes with $K_p \sim 10^4 \text{ M}^{-1}$. Though this cannot be compared to isolated peptides TCAM, TMM, and electrostatically similar control peptide MG(–) because they do not bind strongly enough to permit the calculation of a partitioning coefficient, membrane binding of the TCAM/TMM mixture is nearly an order of magnitude greater than that of MG-12W ($K_p = 1052 \text{ M}^{-1}$), which has an additional positive charge to drive electrostatic binding. Again, this is indicative of cooperative peptide–surface partitioning and molecular recognition between the TCA and TM modules. Nonlinearity in the electrostatically driven binding plot was expected because of the loss of surface potential as the titration experiment progressed. However, the low surface potential of the 10% POPG membrane limited this effect, resulting in relatively linear binding plots for the isolated peptides and moderate nonlinearity at low free-peptide concentrations of the TCAM/TMM mixture (Figure 5C). Thus, fitting the whole data set or just the low free-peptide regime yielded similar partitioning coefficients for the mixture, from 10 000 to 26 000 M^{-1} , is still a marked enhancement over 1052 M^{-1} for MG-12W, which lacks any directed assembly motifs such as the TCA and TM modules. The magainin variants bearing six cyanuric acid and melamine recognition motifs (HCA and HMM, respectively) exhibited strong interactions with each other, even in solution, rendering the membrane-binding experiment impossible because of precipitation upon peptide mixing in any context, whether the lipid vesicles were present or not. However, it was possible to examine the binding between the lipid-anchored TCA module (TCA-PE) and both TMM and HMM. Whereas the surface binding of the isolated TMM and HMM peptides to low potential membranes

(2 and 10% POPG/ePC) was weak, binding to vesicles with 2% TCA-PE/ePC was robust and comparable to binding observed with the TCAM/TMM mixture to 10% POPG/ePC (Table 1). The calculated partitioning coefficients for TMM and HMM to 2% TCA-PE/ePC membranes are ~ 6000 and 3000 M^{-1} , respectively. Electrostatic peptide binding is not detectable at 2% surface charge; thus the initial steps of peptide insertion into the membrane are driven mostly by molecular recognition between cyanuric acid and melamine binding between lipid and peptide. All of the peptide systems in Table 1 exhibit surface saturation with an increasing lipid-to-peptide ratio; however, the selective nature of TMM and HMM binding to TCA-PE membranes is best observed by plotting fractional peptide binding as a function of the TCA-PE/peptide mole ratio (Figure 5D). Interestingly, whereas TMM binding appears to saturate at a TCA-PE/TMM ratio 2, HMM binding saturates at a TCA-PE/HMM ratio 4. Under these conditions a majority of the peptide is surface-bound. A 2:1 binding stoichiometry for TCA-PE/TMM is reasonable if there is a random distribution of the TCA-PE lipid between the inner and outer monolayers of the lipid vesicles; thus only half of the total TCA-PE in the system is available for 1:1 binding with TMM. The 4:1 stoichiometry of TCA-PE and HMM is similarly consistent with only half the total TCA-PE being available on the outer monolayer and further suggests a 2:1 binding between the TCA module and the HMM peptide, as opposed to the 1:1 binding between TCA and TM modules. This is what one would expect if the 1:1 cyanuric acid to melamine binding ratio is maintained, and indeed this appears to be the case. Therefore, despite the drastically different scaffolds used to present cyanuric acid and melamine in the binding of TCA-PE with HMM (Figure 2), a selective binding interaction occurs that preserves the 1:1 binding stoichiometry dictated by the CA/M hydrogen bonding patterns. Further implied in these data is that peptide–surface binding is not accompanied by membrane translocation of the peptide or transmembrane lipid flipping, which should lead to 1:1 binding stoichiometry in all binding experiments.

Membrane Permeation Triggered by Peptide–Peptide and Peptide–Lipid CA/M Recognition. Cooperative binding at the interface translates into enhanced function as well. When assayed for membrane permeation using a calcein release experiment, the 1:1 mixture of TCAM/TMM again displayed greatly enhanced lytic behavior as compared to equimolar treatments with the isolated peptides (Figure 6). The peptide-mediated release of encapsulated dye from 10% POPG vesicles was dose-dependent for all peptides; interestingly, magainin disulfide

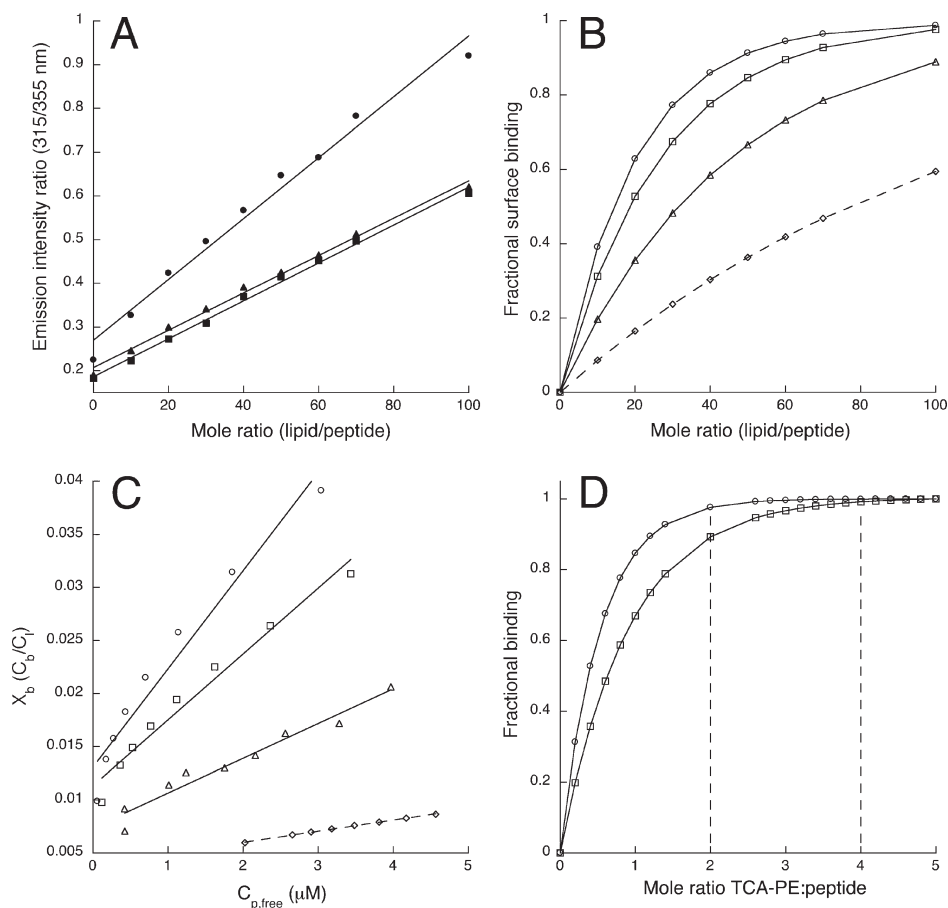


Figure 5. Peptide–membrane partitioning analyses based on tryptophan emission ratios at 315 and 355 nm. (A) Peptides TMM (●), TCAM (▲), and MG-12W (■) bound to 10% POPG/ePC vesicles without approaching surface saturation whereas (B) peptide mixture TCAM/TMM (○) and MG-12W (◇) displayed surface-saturating signals to the same membrane; peptides TMM (□) and HMM (△) also displayed surface saturation when binding to 2% TCA-PE/ePC vesicles. (C) Surface concentration (X_b) of TCAM/TMM (○), MG-12W (◇), TMM (□), and HMM (△) partitioning to vesicles described in panel B as a function of solution peptide concentration; the slope indicates the partitioning coefficient, K_p . (D) Fractional surface binding of TMM (○) and HMM (□) to 2% TCA-PE/ePC vesicles as a function of the TCA-PE/peptide ratio with approximate saturation ratios for TMM and HMM indicated at mole ratios of 2 and 4.

Table 1. Peptide–Membrane Partitioning Coefficients

peptide(s)	membrane	K_p (M^{-1})
MG-12W	10% POPG/ePC	1052
HMM	2% TCA-PE/ePC	3273
TMM	2% TCA-PE/ePC	6199
TCAM/TMM	10% POPG/ePC	9245

homodimer MG-SS displays similar activity at a third of the concentration of the TCAM/TMM mixture. This is expected for two reasons: (1) the noncovalent recognition between TCA and TM modules does not approach that of a covalent bond, so the benefits of preassembly should be far greater for the disulfide-linked dimer and (2) MG-SS is more positively charged than the TMM and TCAM variants so surface binding is inherently superior. Though the membrane aggregation state of the both covalent (MG-SS) and noncovalent (TCAM/TMM) systems in the membrane is unknown, the functional similarity of the two systems is suggestive of a low oligomerization state mediated by peptide–peptide interactions. We expect extensive TCA/TMM noncovalent polymerization at the surface to result in greater membrane activity than for dimer MG-SS.

Prior studies indicated that the tris-melamine magainin conjugate (TMM) can act as a fusion catalyst^{51,52} to merge negatively charged vesicles with those displaying TCA-phospholipid (TCA-PE).⁵⁰ We examined the functional binding of TMM with TCA-

PE and found that the cyanuric acid/melamine interaction is sufficiently robust to drive the lytic insertion of the cationic magainin peptide into membranes with nearly neutral surface potential. In contrast to the binding analysis of TMM or HMM to TCA-PE membranes, the dependence of dye release on the TCA-PE lipid-to-peptide ratio reveals no functional saturation behavior at the 2:1 or 4:1 ratios observed in the binding curves for TMM and HMM, respectively (Figure 5). In fact, maximal membrane permeation is observed only when excess TMM or HMM to TCA-PE is used (Figure 6). This puzzling result becomes more meaningful upon consideration of the partitioning coefficients K_p of ~ 6000 and $3000 M^{-1}$ for TMM and HMM (Table 1), respectively, and the total lipid concentration of $50 \mu M$. The ratio of surface-bound peptide to free peptide in solution is given by the relationship

$$K_p = \frac{C_B/C_L}{C_{p, \text{free}}}$$

Because $C_L K_p = C_B/C_{p, \text{free}}$, the expected ratios of bound peptide to solution-phase peptide are 0.3 and 0.15 for TMM and HMM, respectively. Therefore, under these experimental conditions, the majority of peptide is in solution, and only one-sixth to one-third of the total peptide concentration is calculated to be surface-bound, obscuring the lytic effect of surface-saturated peptide binding. Increasing lipid concentration results in a loss of the

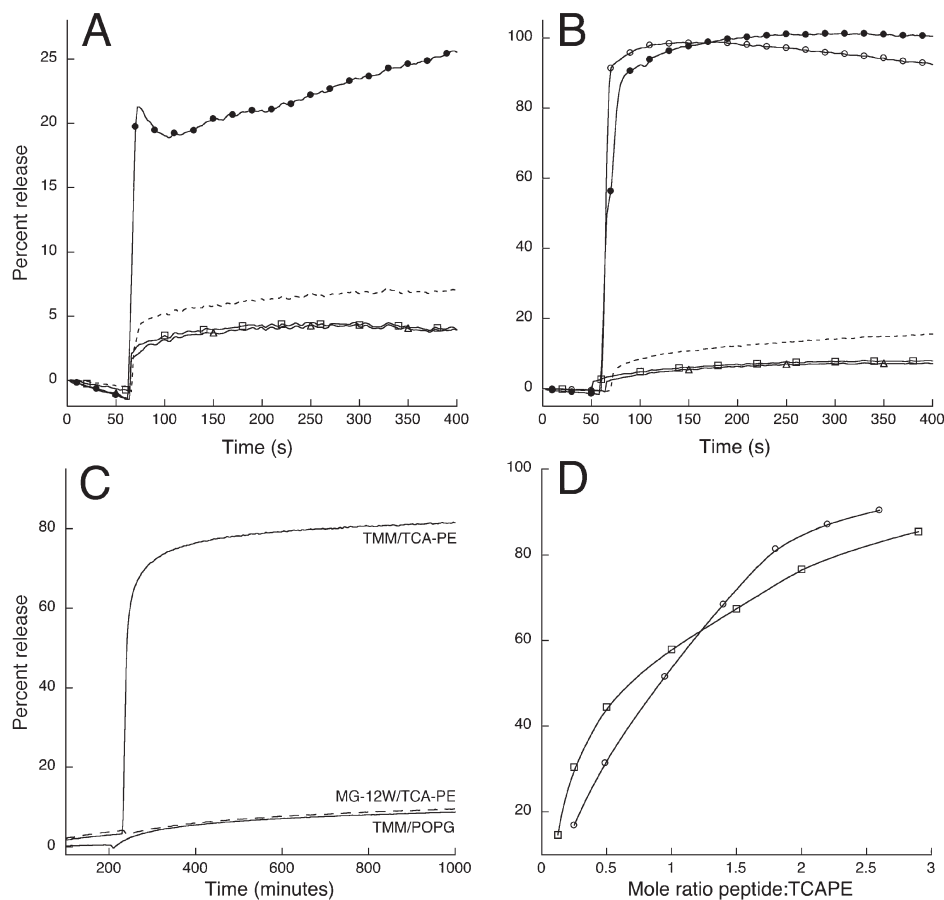


Figure 6. Percent calcein dequenching release from 10% POPG/ePC vesicles (total lipid concentration of 50 μM) upon treatment with TCAM/TMM (●), MG-12W (---), TMM (□), and TCAM (Δ) at (A) 1 μM and (B) 3 μM total peptide concentrations. Release effected by 0.5 μM MG-SS disulfide (1 μM peptide anchor) (○) is shown in panel B as well. (C) Percent carboxyfluorescein dequenching release from 2% TCA-PE/ePC vesicles or 2% POPG/ePC vesicles effected by magainin variants as indicated. (D) Dequenching dye release from 2% TCA-PE/ePC vesicles as a function of the peptide/TCA-PE mole ratio where the peptide is TMM (○) or HMM (□).

signal-to-noise ratio for dye release, preventing observation under surface-saturating peptide binding. However, it is clear that molecular recognition between cyanuric acid and melamine modules can enhance both membrane binding and permeation.

Conclusions

We have demonstrated herein that designed molecular recognition between cyanuric acid and melamine modules enhances both binding and permeation of magainin peptide derivatives. Magainin binding to membranes is directed by complementary electrostatic interactions between peptide and surface. These systems were investigated at the lowest possible surface charge to permit a clear observation of the effects of designed peptide recognition between pendant CA/M groups. Indeed, under these conditions, enhanced binding and func-

tionality was observed only when both recognition groups and the membrane were present. Notably, the self-assembling magainin peptide systems exhibited weaker but comparable permeation activity with respect to that of covalently dimerized peptide MG-SS, suggesting that designed noncovalent interactions may be a reasonable avenue to pursue in the development of new surface-active agents.

Acknowledgment. This work was supported in part by the NSF (NSF-0747194, NSF-927778) and the Institute of Materials Research at The Ohio State University.

Supporting Information Available: Detailed synthesis procedures and compound characterization and additional CD and fluorescence spectra. This material is available free of charge via the Internet at <http://pubs.acs.org>.